J. Fluid Mech. (2010), *vol.* 650, *pp.* 415–425. © Cambridge University Press 2010
doi:10.1017/S0022112010000583

Hovering of a rigid pyramid in an oscillatory airflow

ANNIE WEATHERS[1], BRENDAN FOLIE[2], BIN LIU[3]†, STEPHEN CHILDRESS[3] AND JUN ZHANG[1,3]

[1]Department of Physics, New York University, 4 Washington Place, New York, NY 10003, USA

[2]Department of Mathematics, Harvey Mudd College, 301 Platt Boulevard, Claremont, CA 91711, USA

[3]Applied Mathematics Laboratory, Courant Institute, New York University, 251 Mercer Street, New York, NY 10012, USA

(Received 9 September 2009; revised 27 January 2010; accepted 30 January 2010; first published online 19 March 2010)

We investigate the dynamics of rigid bodies (hollow 'pyramids') placed within a background airflow, oscillating with zero mean. The asymmetry of the body introduces a net upward force. We find that when the amplitude of the airflow is above a threshold, the net lift exceeds the weight and the object starts to hover. Our results show that the objects hover at far smaller air amplitudes than would be required by a quasi-steady theory, although this theory accounts qualitatively for the behaviour of the system as the body mass becomes small.

1. Introduction

Reciprocal motion is common in the biological world, and is especially evident in the forward flapping flight and hovering of birds and insects (see Vogel 1996; Dudley 1999; Alexander 2002). At high Reynolds numbers, hovering flight is associated with the shedding of vortical structures from the wings, resulting in a downward momentum flux (see Ellington 1984). The experiment reported here is meant to simulate the dynamics of reciprocal locomotion by subjecting a free object to an oscillating background flow of air. The analogy depends on the similarity between the vortical structures shed in active flapping, and those created by the movement of the background flow relative to the passive object. Childress, Vandenberghe & Zhang (2006) have shown that a flexible body, driven passively in a background airflow oscillating vertically with no mean component, is able to hover stably. The body has a built-in asymmetry that, together with the induced flapping motion, leads to the shedding of vortex dipoles and the production of net lift. Another example of a shape-changing body subject to an oscillating viscous flow is studied numerically by Spagnolie & Shelley (2009), where a body can hover or ascend with a similar structure of shed vortices.

Although flexibility is a necessary property of an object capable of active flapping, a rigid passive object is in principle able to shed vorticity in an oscillating flow field. If the object has sufficient up–down asymmetry, the possibility arises that hovering could be achieved without flexing, simulating, in effect, active flapping at small amplitude about a fixed rest state. As an extension of the research reported in Childress *et al.* (2006), we consider here the hovering of geometrically similar objects – rigid hollow

† Email address for correspondence: binliu@cims.nyu.edu

https://doi.org/10.1017/S0022112010000583 Published online by Cambridge University Press

paper 'pyramids' – of varying sizes and masses. By adjusting the amplitude of the oscillating background airflow, the onset of hovering can be measured. We shall show that flexible and rigid bodies hover at comparable flow amplitudes, provided that sufficient up–down asymmetry is present. Our results suggest that, at sufficiently large frequency, large-wing amplitudes are not necessary for the production of lift by active flappers. The lift produced in our experiment is found to be significantly larger than would be deduced from a quasi-steady theory based upon form drag in steady flows. Quasi-steady theory is successfully used, however, to estimate the qualitative effect of reducing the mass of the hovering object.

In our ongoing research, the phenomena is being explored further in two dimensions, using visualization in a water tank of the vorticity shed by a V-shaped object. Also, a two-dimensional model for lift production similar to that used in Childress *et al.* (2006) is being pursued. The results of this work will be reported elsewhere.

2. Experimental results

2.1. *Experimental set-up*

The oscillating background air is supplied by an alternating current (AC) wind tunnel, composed of a large speaker, above which sits a 15 cm diameter test section (see figure 1). The strength of the oscillating wind can be adjusted by varying the amplitude and the frequency f of the sinusoidal signal driving the speaker. The peak-to-peak displacement A of the airflow is calibrated by obtaining the peak-to-peak amplitude of a light piston (made of styrofoam) hanging in the middle of the test section. The piston is driven passively by the airflow and oscillates at the same frequency. The air amplitude can thus be measured using a high-speed camera. The relative phase of the piston and the input signal can also be obtained. We vary the frequency from 10 to 30 Hz. The amplitude of the oscillating air A can reach 10 cm at a fixed frequency.

The pyramids are constructed of wax paper, which is folded as shown in the inset of figure 1; they typically measure a few centimetres in length. Carbon fibres are attached to the edges of the paper pyramid to act as a frame to maintain its rigidity in the presence of the high-speed airflow (up to $2\,\mathrm{m\,s^{-1}}$). The pyramid shape was chosen as an easily fabricated geometry providing the necessary asymmetry. The geometry of such objects can be varied by changing the height-to-width ratio, which we specify in terms of the apex angle θ, the angle between any of its triangular surfaces and its axial line. The weight of such pyramids can be increased by evenly winding thin metallic wires along the carbon fibre frame. In order to prevent the lateral motion of the object as it hovers in the airflow, the object is allowed to slide along a steel guide wire standing vertically in the centre of the air chamber, through a small hole cut through the top of the pyramid. The friction between the pyramid and guiding wire is negligible compared to the typical drag of the pyramid.

2.2. *Criterion for hovering of an object of various sizes*

The net lift on an object due to an oscillating background airflow is a function of the Reynolds number

$$Re = fAa/\nu, \tag{2.1}$$

where f, A and ν are respectively the frequency, amplitude and kinematic viscosity of the airflow, and a is the characteristic length of the object. In an extremely slow oscillating flow, when the Reynolds number is small and the inertia of the fluid is negligible, the object experiences a zero net force over a period of air oscillation (see

https://doi.org/10.1017/S0022112010000583 Published online by Cambridge University Press

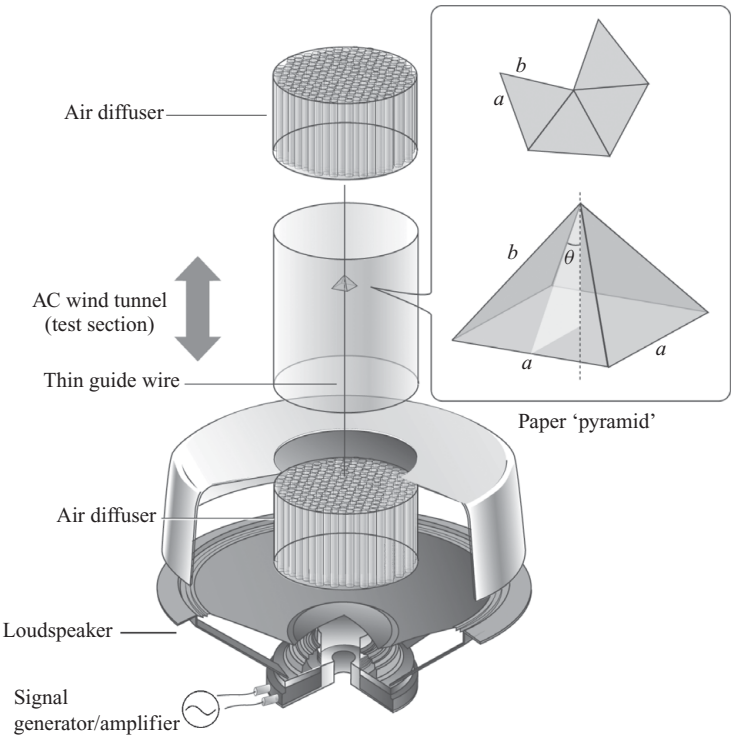


FIGURE 1. Experimental set-up. An AC air current is generated by a loudspeaker, 42 cm in diameter, driven sinusoidally by a signal generator and an amplifier. The oscillating airflow in the vertical tube has a zero mean, operating at controlled frequency ($10 \sim 30$ Hz) and amplitude ($1 \sim 10$ cm). A hollow 'pyramid' (inset), measuring a few centimetres, can be driven passively in this AC wind tunnel. The pyramids are made with folded wax paper. The rigidity is provided by supporting frames made of thin carbon fibre rods. The passively driven rigid body is allowed to move only vertically, sliding along a thin steel rod. The friction due to the sliding is found to be negligible compared to the form drag.

Purcell 1977). In this case, the flow is governed by the linear Stokes equations, where the drag is a linear function of the velocity and can therefore have no non-zero mean. In particular, the drag is invariant under flow reversal, independent of any up–down asymmetry. On the other hand, at large Reynolds numbers the vertical drag force F_D varies with the direction of the airflow past the body. When the difference in vertical drag is greater than the weight of the object, the object can be lifted up against gravity. We remark that we are using here the language of quasi-steady fluid flow, even though in our experiment the velocity is oscillatory with zero mean and hence fundamentally unsteady.

Our experimental results agree with the above arguments. At relatively low speeds of the oscillating air, characterized by the product of its frequency and amplitude (fA), the pyramid remains on the bottom of the chamber with the peak air drag less than its weight. As the peak air speed is further increased, the object becomes partially entrained by the flow, periodically lifted, and then returned to the bottom of the chamber. Above a critical value, the pyramid detaches completely from the bottom and abruptly begins to ascend. The hovering equilibrium (lift = weight) is, in principle, invariant under a constant vertical velocity (Dabiri 2005); however, in our experiment the 'state' of the hovering body varies with its ascent velocity and is adjusted by the

https://doi.org/10.1017/S0022112010000583 Published online by Cambridge University Press

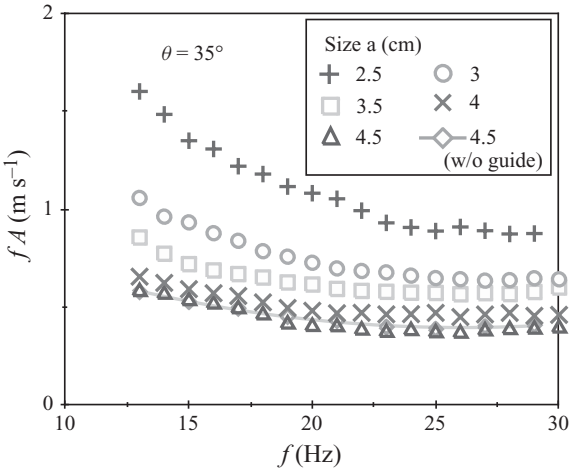


FIGURE 2. The minimum peak air speed fA required for pyramid-shaped objects of various sizes to hover at a frequency f. The mass of the objects is fixed at $m = 0.215$ gm, and its shape is fixed with $\theta = 35°$. As a comparison, the air speed required for free hovering without the guiding wire is shown by the connected curve of 'diamonds', demonstrating a minimal effect of the wire.

air amplitude. This situation is evident in the quasi-steady model below. In practice, fine tuning of the amplitude can move the pyramid to a predetermined height, because of slight vertical variation of the conditions within the chamber. Hovering at this reference altitude determines a critical amplitude.

The minimum air speeds fA required for pyramids of various sizes (a varies from 2.5–4.5 cm) are shown in figure 2. Free hovering data without the guide wire is also plotted, and the effect due to the friction is minor. For each pyramid, the lower the air frequency, the higher the air speed required for it to hover. At fixed frequency and fixed mass, pyramids of larger size require less air speed to hover. Since Re in our experiments always exceeds 500, the phenomena reported here should be regarded as being in the high-Re regime.

2.3. *Quasi-steady model*

In spite of the fundamental unsteadiness of our problem, it is helpful to invoke a quasi-steady model to gain some idea of the mechanics of the system. The difference of the drag due to the upward and downward motion of such a pyramid is dependent on the up–down asymmetry of the hovering object, which can be quantified by the fluid drag experienced in a steady flow. When an object with projected area S moves with velocity u relative to a fluid of density ρ, the steady fluid drag may be expressed as (see Batchelor 1967):

$$F_D = \frac{1}{2}\rho u^2 C_D S. \tag{2.2}$$

Here C_D is the drag coefficient, a dimensionless number dependent on the geometry of the object relative to the flow direction. C_D is observed to be roughly independent of Re for many objects when Re is sufficiently high, i.e. $Re \gtrsim 500$ (Batchelor 1967). The drag coefficients of the pyramids can be obtained from (2.2) by measuring the terminal velocity V in free fall. The free object, falling at a speed of order $1\,\mathrm{m\,s^{-1}}$ with $Re = Va/\nu$ of order 10^3, is photographed with a high-speed camera. The drag coefficients in the two possible orientations can be thus measured.

https://doi.org/10.1017/S0022112010000583 Published online by Cambridge University Press

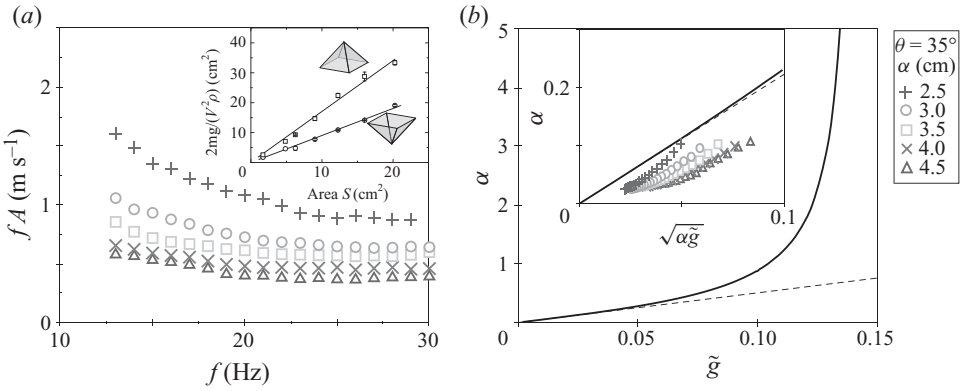


FIGURE 3. Asymmetric air drag and its consequent criterion for hovering. (*a*) The drag coefficients C_D of the paper pyramids of various projected areas S for a similar shape ($\theta = 35°$), obtained by measurements of terminal speed V in free fall as the drag balances with the weight mg. Two orientations give rise to different drag coefficients (slopes of the two straight lines) as they fall. (*b*) The computed criterion for hovering, $\alpha(\tilde{g})$, based on the quasi-steady approximation of the fluid drag, with the drag coefficients derived from (*a*) being applied. α is the dimensionless measure of the air amplitude, while $\tilde{g}$ is the dimensionless acceleration due to gravity. The inset shows the critical dimensionless amplitude α against the dimensionless period $\sqrt{\alpha\tilde{g}}$ and includes the data sets of figure 2. The dashed lines are the tangents at $\alpha = 0$.

As shown in figure 3(*a*), the drag force in terminal free fall ($F_D = mg$) of pyramids with similar geometry ($\theta = 35°$) is proportional to the projected area S and the square of its terminal velocity. The two data sets for $2F_D/V^2\rho$ are plotted against the projected area S for the two possible orientations. The measured slopes yield the drag coefficients $C_D^+ = 1.7$ and $C_D^- = 0.9$, with $\Delta C_D = C_D^+ - C_D^- = 0.8 \pm 0.1$.

Considering an oscillating background air with its peak-to-peak displacement A, the velocity of the air can be expressed as a sinusoidal function as $u = \pi f A \sin(2\pi f t)$. The net drag on a fixed pyramid immersed in such an oscillating air flow can be approximated by averaging the steady drag (see (2.2)) over the entire period $T = 1/f$:

$$\langle F_D \rangle = \frac{1}{2}\rho S \frac{1}{T}\left(\int_0^{T/2} \mathrm{d}t C_D^+ u^2 - \int_{T/2}^{T} \mathrm{d}t C_D^- u^2\right) = \frac{\pi^2}{8}\rho S\left(C_D^+ - C_D^-\right) f^2 A^2. \qquad (2.3)$$

Only when this quantity is large enough to balance the weight can a free object hover.

In the quasi-steady model the condition is applied as follows. The position $Y(t)$ of a fixed point on a pyramid satisfies

$$\frac{1}{2}\sigma\rho(U - \dot{Y})^2 S C_D^\sigma = M\ddot{Y} + mg, \qquad (2.4)$$

where $U(t)$ is the oscillating background flow, $\sigma = \mathrm{sgn}(U - \dot{Y})$, M is the sum of the mass m and virtual mass m_v of the pyramid. We may estimate m_v conservatively to be $\rho a^3 \sim 0.01$ gm, which is negligible compared to the mass m for the data of figure 2. If we set $t = \phi/2\pi f$, $U = \pi f A \sin\phi$, $Y = Ay/2$, the dimensionless form of the equation becomes

$$\frac{\mathrm{d}^2 y}{\mathrm{d}\phi^2} = \alpha\sigma C_D^\sigma\left(\sin\phi - \frac{\mathrm{d}y}{\mathrm{d}\phi}\right)^2 - \tilde{g}. \qquad (2.5)$$

https://doi.org/10.1017/S0022112010000583 Published online by Cambridge University Press

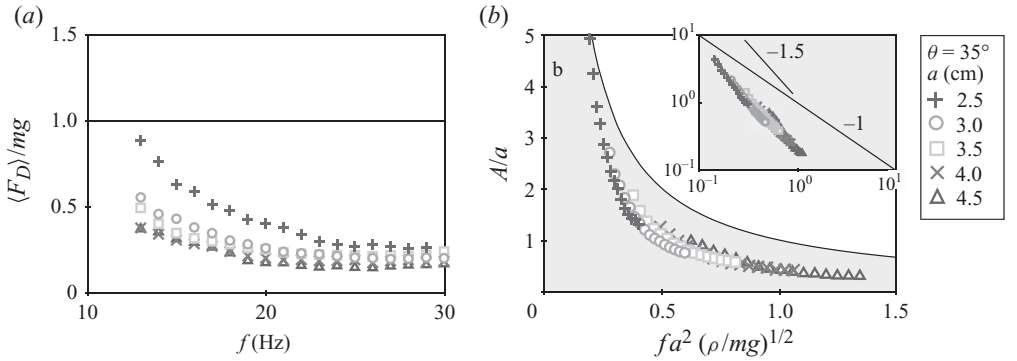


FIGURE 4. Comparison between the criterion for hovering obtained experimentally and that given by the quasi-steady solution. The paper pyramids are of similar shape with $\theta = 35°$, with the mass fixed at $m = 0.215$ gm. (*a*) Using (2.3), the lift calculated from measured airflow at hovering, using the quasi-steady model, is much less than the weight of the pyramid. (*b*) The data points show the experimental measurement of the dimensionless air displacements A/a against the dimensionless air oscillating frequency $fa^2\sqrt{\rho/mg}$ when the pyramid hovers. The solid line, $A/a < 1.0684 \times (fa^2\sqrt{\rho/mg})^{-1}$, shows the criterion for hovering, according to the quasi-steady approximation. Below this line, the lift obtained from the oscillatory airflow cannot support the weight of the paper pyramid. The log–log plot of the experimental results (shown in the inset) suggests a power-law dependence with an exponent more negative than -1, the value obtained in the quasi-steady approximation. The peak required air speeds are significantly less than the quasi-steady values at higher frequencies.

Here $\alpha = (1/4)(\rho SA/M)$, $\tilde{g} = (m/M)(g/(2\pi^2 f^2 A))$. Note that α is a dimensionless measure of air amplitude, while $\tilde{g}$ is the dimensionless weight of the paper pyramids. By solving (2.5) numerically, we find that, given a dimensionless weight $\tilde{g}$, there is a critical dimensionless air amplitude α, above which the mean speed of the pyramids is nonnegative. This critical α gives the criterion for hovering. The parameter $\beta = 1/\sqrt{\alpha\tilde{g}}$, which is independent of A, will also be useful. The numerical calculations yield α as a function of $1/\beta$ as shown in figure 3(*b*). From this we may deduce from the tangent line at the origin the inequality $\alpha \geqslant 5.0\tilde{g}$. Since the asymptotic behaviour for small α and large β corresponds to high-frequency small-amplitude air oscillation, the inequality coincides with the relation obtained by neglecting the term $\mathrm{d}y/\mathrm{d}\phi$ in (2.5). Setting $S = a^2$, the criterion for hovering in this approximation yields the inequality

$$A/a \geqslant \frac{2\sqrt{2}}{\pi}\sqrt{\frac{1}{C_D^+ - C_D^-}}\left(fa^2\sqrt{\frac{\rho}{mg}}\right)^{-1}. \tag{2.6}$$

A related simplified criterion for hovering, using piecewise constant airflow but retaining the body motion, is given in Spagnolie (2008). The dimensionless variable A/a is the ratio of the air displacement to the size of the pyramid. The dimensionless oscillating frequency, $fa^2\sqrt{\rho/mg}$, combines a Froude number with a mass ratio.

In figure 4, we compare the quasi-steady results with the minimal hovering flow velocity for pyramids of the same weight (0.215 gm) and fixed geometry $\theta = 35°$. Based on the steady air drag (see (2.2)), the potentially supportable hovering weight of the pyramid is found to be much smaller than the actual weight of the hovering pyramids, as shown in figure 4(*a*), especially for higher air frequency and larger pyramid size. In figure 4(*b*), the hovering criterion measured experimentally is shown in the form of A/a as a function of $fa^2\sqrt{\rho/mg}$. We superimpose the quasi-steady hovering criterion

https://doi.org/10.1017/S0022112010000583 Published online by Cambridge University Press

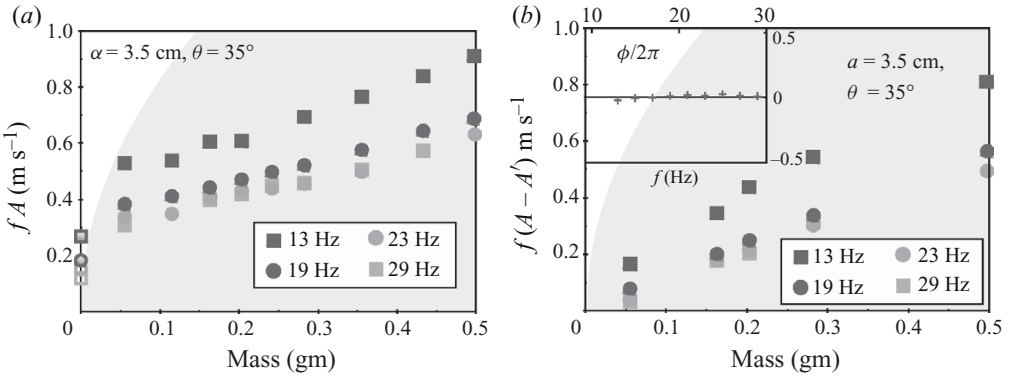


FIGURE 5. Dependence of the minimal flow velocity fA on hovering mass. The shadowed area shows the regimes excluded by the criterion for hovering based on (2.6). (*a*) With the oscillating frequency fixed, the dependency of hovering mass on the experimentally measured peak air velocity suggests a linear response, as shown by the solid data points. The hollow symbols at $m = 0$ show the finite minimum air speed required for a paper pyramid of vanishing mass (sufficiently greater than the virtual mass) to hover, which is obtained by the quasi-steady approximation. At a fixed mass, the experimentally measured peak air speed fA, required for objects with a fixed shape ($a = 3.5\,\text{cm}$, $\theta = 35°$) to hover decreases and tends to saturate as the frequency f increases. The data sets are for several values of their frequencies. (*b*) Dependence of the relative peak air speed $f(A - A')$ on the hovering mass, where A' is the peak to peak amplitude of the hovering object measured experimentally. The inset shows the phase difference ϕ between the displacement of the air and the displacement of the body, for a body having $m = 0.203\,\text{gm}$, as a function of frequency.

$A/a \geqslant 1.0684(fa^2\sqrt{\rho/mg})^{-1}$ obtained from (2.6). We see that these variables collapse the data over the range of sizes studied here. It is revealing that the experimental data falls well below the lower bound obtained from the quasi-steady approximation, except at very low frequencies. The log–log plot of A/a against $fa^2\sqrt{\rho/mg}$ (inset in figure 4) shows a power-law dependence with an exponent of about -1.5, compared to the value of -1 expected from the quasi-steady approximation.

2.4. *Hovering capability as a function of mass*

For fixed size and geometry, a lighter object requires less relative air speed to hover since less drag is necessary to balance the weight. However it is not clear how fA varies with the mass. As we show in figure 5(*a*), the required peak air speed for hovering, fA, decreases almost linearly with the mass at a fixed frequency f. In these measurements the size and geometry of the pyramid is fixed at $a = 3.5\,\text{cm}$, $\theta = 35°$; the drag coefficient difference is the same as above, $\Delta C_D = 0.8$. Surprisingly, the minimal flow velocity does not seem to extrapolate to zero for small mass. This suggests that an object does not necessarily hover in a weak oscillating background flow as it becomes neutrally buoyant. Instead, the object still requires a finite amount of peak air speed to generate the necessary lift, at least so long as body mass is large compared to the virtual mass. In the studies reported in Spagnolie & Shelley (2009), the importance of significant mass to the 'ratcheting' of the body was also observed.

A criterion for an object to hover at small mass can be obtained from the quasi-steady approximation (2.4). For completeness we retain the small virtual mass, which has been considered by Kanso *et al.* (2005) for vanishing body mass. Then, with m

https://doi.org/10.1017/S0022112010000583 Published online by Cambridge University Press

and m_v small, we must conclude that $\dot{Y} \to U$, so that

$$\frac{1}{2}\sigma\rho(U-\dot{Y})^2 S C_D^{\sigma} \approx (m+m_v)\dot{U} + mg. \tag{2.7}$$

It follows that $v \equiv U - \dot{Y}$ has the same sign as $(m+m_v)\dot{U} + mg$. Solving, $v = -k\sqrt{|(m+m_v)\dot{U}+mg|/C_D^-}$ where it is negative, and $v = k\sqrt{((m+m_v)\dot{U}+mg)/C_D^+}$ where it is positive, k being a common constant, defined as $k = \sqrt{2m/\rho S}$. The condition for hovering then yields $2\pi^2 f^2 A((m+m_v)/m) = 6.93g$, or $fA = 0.351(gm/f(m+m_v))$. The theory thus correctly represents the decrease of the extrapolated, small mass values in figure 5 with increasing frequency at body masses large compared to the virtual mass, although the limiting values obtained with $m_v = 0$ are somewhat smaller. As the mass falls below the virtual mass, fA does drop towards zero. Note that the quasi-steady inequality (2.6) here gives the condition $fA \geqslant 2.6\sqrt{m}\,\mathrm{m\,s^{-1}}$, but this becomes exact only for small α, whereas we see that α diverges for small m and m_v. The shaded area in figure 5 shows the values excluded by this inequality, although we cannot usefully extend them to the origin.

From these calculations we can deduce that the reason for a finite hovering speed at near zero mass comes from the reduction in the 'relative' velocity as mass is reduced. The body is increasingly entrained in the flow, with the result that a finite air amplitude must be maintained to insure the vanishingly small relative velocity needed for lift. The dependence of the 'relative' peak air speed on the mass of the hovering object was verified experimentally and the data is shown in figure 5(*b*). In the inset one sees that the phase difference between the pyramid and the oscillating air is very small, showing the entrainment of the hovering object at various air frequencies. As a consequence, the relative air speed can be represented by the peak-to-peak value of $f(A-A')$, where A is the air displacement and A' is the object displacement. When the mass of the pyramid approaches zero, the relative air speed is seen to also approach zero. We emphasize that our measurements stop short of masses comparable to the probable virtual mass. The domain excluded by the quasi-steady criterion is again shown as the shaded area.

2.5. *Dependence on geometry*

For pyramids of fixed mass and fixed projection area, the minimal flow velocity to hover also depends on its apex angle θ. Here we vary the pyramid geometry by modifying the angle θ while keeping the weight as well as the projected area $A = a^2$ fixed. A value of θ equal to 90° corresponds to a plane square, while a value of θ near 0° corresponds to a long thin structure. The dependence of the minimal flow velocity upon the apex angle θ is shown in figure 6. The inset shows the drag coefficients of pyramids of varying geometry, again obtained from the terminal velocity in free fall. As θ approaches 90°, the object requires a relatively high air speed to hover as all asymmetry is lost. As θ decreases, the difference between the two drag coefficients ΔC_D increases due to the increasing spatial asymmetry. At fixed weight, the minimum required air speed therefore decreases. For yet smaller values of θ, the minimum required air speed starts to increase as the up–down asymmetry becomes less pronounced. There appears to be an optimal geometry with its apex angle $\theta \sim 30°$, independent of the oscillating frequency. The height of such an optimal shape is about the same as its lateral size a.

https://doi.org/10.1017/S0022112010000583 Published online by Cambridge University Press

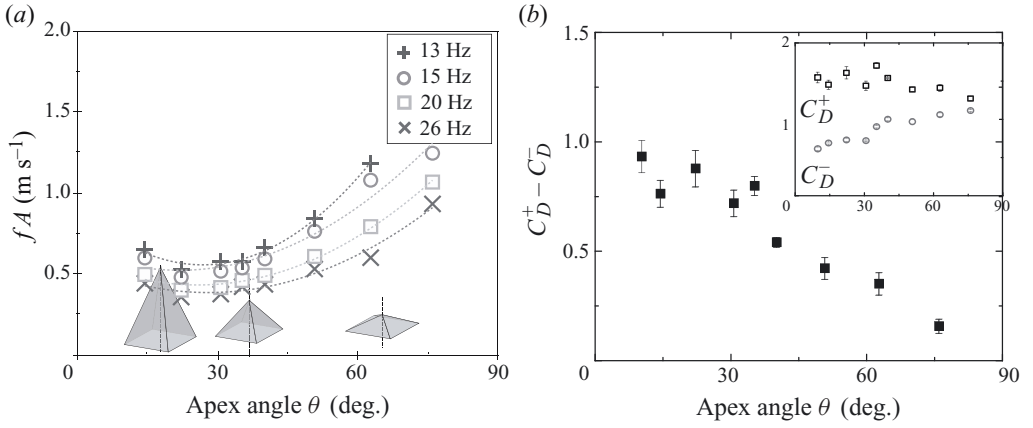


FIGURE 6. (*a*) Dependence of the required air speed on the geometry of the hovering pyramids, for various frequencies. An optimal shape of the rigid pyramid is observed with an apex angle $\theta \sim 30°$, where the lowest air speed is needed. (*b*) The dependence of the drag coefficients on θ is also shown.

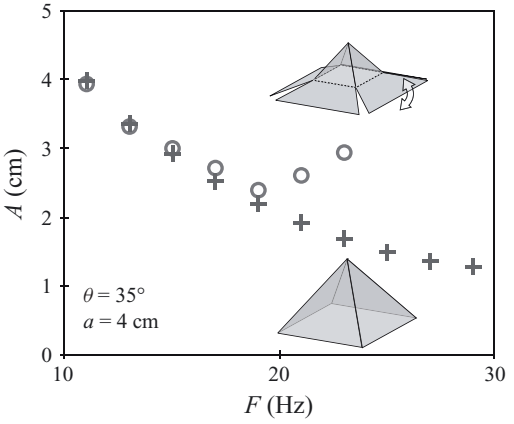


FIGURE 7. Comparison of hovering between the flexible and the rigid pyramids of the similar shape. Their shape and mass are fixed at $a = 4$ cm, $m = 0.153$ gm. The upper and lower data sets correspond to a flexible and a rigid pyramid respectively, as shown by the insets besides the data sets.

3. Rigid versus flexible bodies

It is of interest to compare the present results for rigid objects with the measurement of hovering of flexible bodies in an oscillating flow, as reported by Childress *et al.* (2006). We now consider a comparison of hovering of similar paper pyramids with and without flexibility. The flexibility is realized by making a paper pyramid of the same shape, however, with the vertex lines cut halfway towards its top. Therefore its sidewalls are able to flap along the folding line (see figure 7). As shown in figure 7, the flexible and rigid pyramids are found to require almost the same air amplitude in order to hover. This suggests that similar mechanisms of vortex shedding prevail. As the oscillating frequency f increases, the rigid paper pyramids hover more easily than the flexible one. There appears to be a clear optimal frequency for the flexible

https://doi.org/10.1017/S0022112010000583 Published online by Cambridge University Press

pyramids, obtaining minimal flow amplitude (cf. Childress *et al.* 2006), while the rigid one, if it does reach a minimum amplitude, does so at a much larger frequency.

4. Discussion

A pyramid-shaped object is observed to hover freely in an oscillating background air flow with zero mean component, provided that the amplitude of the oscillation is sufficiently large. The required amplitude depends on the body size and geometry, as well as its mass. A quasi-steady theory may be used to obtain a criterion for hovering. This theory involves three dimensionless parameters: the dimensionless air displacement A/a, the dimensionless oscillating frequency fa^2/ν and the dimensionless mass $mg/\rho\nu^2$. If it is assumed that the large Reynolds number of our experiment eliminates the dependence upon ν, then the relevant parameters are A/a and $fa^2\sqrt{\rho/mg}$. Our data for pyramids of fixed weight for the hovering value of A/a, as a function of the above frequency parameter, nicely collapses the influence of size.

Our investigation reveals a large overestimate of the hovering amplitude given by the quasi-steady approximation. Also, preliminary results suggest that flexibility can play a minor role in determining the minimal hovering amplitude. Taken together, our observations suggest that some rigid bodies, suspending in oscillating air, mimic the vortex shedding associated with active flapping. That is to say, our experiment may model active flapping with little wing movement, which could provide a surprisingly effective hovering mode. It is interesting that Altshuler *et al.* (2005) have observed short-amplitude high-frequency hovering in honeybees, with the unsteady mechanism during its stroke reversal contributing largely to the net upward force.

Our hovering pyramids do not benefit very much from being light. A lighter object can be more easily entrained by the surrounding air, resulting in less relative flow past the free object. For active flappers this translates into similar efforts in terms of wing movement. Body mass may play a key role in determining the efficiency of hovering flight (Spagnolie & Shelley 2009).

Although we have observed an optimal configuration within the family of shapes considered in this report, we have not undertaken any investigations outside of the pyramidal shape. Our hovering amplitudes are comparable to those observed by Childress *et al.* (2006) for a different shape with flexible wings. Perhaps the geometry of the hovering rigid object can be optimized by maximizing the up–down drag asymmetry.

In this paper quasi-steady theory has been used as a benchmark for our experiment. While this theory significantly underestimates the lift provided by the oscillating airflow, it provides the analytical basis for some aspects of the problem, such as the effect of small mass. We have postponed to a subsequent paper the observations and modelling of the shed vorticity responsible for the unsteady lift production. We do not, at present, have a simple physical model that could account for the substantial drag enhancement we observe. However, it is quite possible that an improved drag law, incorporating the effects of acceleration, would lead to hovering amplitudes closer to those observed. Mei (1994) and Odar & Hamilton (1964) have discussed such drag laws for an accelerating sphere. Here the asymmetry of the body is an important feature, which would have to be incorporated into any such improved model. We have dealt in the flexible case with unsteadiness in a simple two-dimensional model (see Childress *et al.* 2006). Although this model qualitatively agreed with much of the experimental data, it did not offer any quantitative comparison with this data. We

https://doi.org/10.1017/S0022112010000583 Published online by Cambridge University Press

surmise that the same situation may prevail for the rigid case, and that ultimately numerical simulation is needed to accurately compute the observed lift.

We thank helpful discussions with S. Spagnolie. This work is supported by DOE (DE-FG02-88ER25053) and NSF (DMS-0507615, DMS-0821520).

REFERENCES

Alexander, D. E. 2002 *Nature's Flyers: Birds, Insects, and the Biomechanics of Flight*. The Johns Hopkins University Press.

Altshuler, D. L., Dickson, W. B., Vance, J. T., Roberts, S. P. & Dickinson, M. H. 2005 Short-amplitude high-frequency wing strokes determine the aerodynamics of honeybee flight. *Proc. Natl Acad. Sci. USA* **102**, 18213–18218.

Batchelor, G. K. 1967 *An Introduction to Fluid Dynamics*. Cambridge University Press.

Childress, S., Vandenberghe, N. & Zhang, J. 2006 Hovering of a passive body in an oscillating airflow. *Phys. Fluids* **18**, 117103.

Dabiri, J. O. 2005 On the estimation of swimming and flying forces from wake measurements. *J. Exp. Biol.* **208**, 3519–3532.

Dudley, R. 1999 *The Biomechanics of Insect Flight*. Princeton University Press.

Ellington, C. P. 1984 The aerodynamics of hovering insect flight. Part I–VI. *Phil. Trans. R. Soc. Lond.* **B305**, 1–181.

Kanso, E., Marsden, J. E., Rowley, C. W. & Melli-Huber, J. B. 2005 Locomotion of articulated bodies in a perfect fluid. *J. Nonlinear Sci.* **15**, 255–289.

Mei, R. 1994 Flow due to an oscillating sphere and an expression for unsteady drag on the sphere at finite Reynolds number. *J. Fluid Mech.* **270**, 133–174.

Odar, F. & Hamilton, W. S. 1964 Forces on a sphere accelerating in a viscous fluid. *J. Fluid Mech.* **18**, 302–314.

Purcell, E. M. 1977 Life at low Reynolds number. *Am. J. Phys.* **45**, 3–11.

Spagnolie, S. E. 2008 Flapping, ratcheting, bursting, and tumbling: a selection of problems in fluid-body interaction dynamics. PhD thesis, New York University, New York.

Spagnolie, S. E. & Shelley, M. J. 2009 Shape-changing bodies in fluid: Hovering, ratcheting, and bursting. *Phys. Fluids* **21**, 013103.

Vogel, S. 1996 *Life in Moving Fluids*, 2nd edn. Princeton University Press.

https://doi.org/10.1017/S0022112010000583 Published online by Cambridge University Press